34th Danubia-Adria Symposium on Advances in Experimental Mechanics
University of Trieste, Italy, 2017

INVESTIGATION OF THE CHIP FORMATION USING HIGH-SPEED CAMERA AND FINITE ELEMENT METHOD

Attila KOSSA[1], Gabor STEPAN[2]

[1] Budapest University of Technology and Economics, Department of Applied Mechanics, Muegyetem rkp. 5., Budapest, 1111 Hungary. E-mail: kossa@mm.bme.hu

[2] Budapest University of Technology and Economics, Department of Applied Mechanics, Muegyetem rkp. 5., Budapest, 1111 Hungary. E-mail: stepan@mm.bme.hu

1. Introduction

Cutting can be considered as one of the most important material removal processes. It is well known, that even small enhancement of a machining process can cause significant cost reduction and quality improvement. Better understanding of the relation between machining parameters (cutting speed, feed rate, depth of cut, etc.) and output variables (cutting forces, temperature field, surface roughness, chip morphology, etc.) could be a key to such improvements. This goal requires the accurate description of the chip formation process.

In the last few decades, significant research effort has been invested into the development of computational methods and their implementations regarding to the simulation of various cutting processes. Researchers widely use the finite element method to analyze various cutting processes. However, it should be emphasized, that there is no agreement how to properly model the cutting mechanisms. Consequently, the results delivered by a finite element analysis (FEA) could be inaccurate. Comparison of the experimental and the numerical results is essential to understand the underlying phenomena.

This article investigates, in detail, the results obtained using FEA compared to the experimental observations for planning processes.

2. Experiments

2.1 High-speed camera recordings

The chip formation processes were recorded using high-speed camera. A Photron Fastcam SA5 775K C3 high-speed camera equipped with a Nikon Nikkor 200mm f/4D AF macro lens was used to capture the chip formation in a planning processes. The setup is illustrated in Fig. 1. Some sample images are shown in Fig. 2. The machining was carried out on a CNC machining center, NCT EmR-610Ms. The material of the specimen was aluminium A2024-T351.

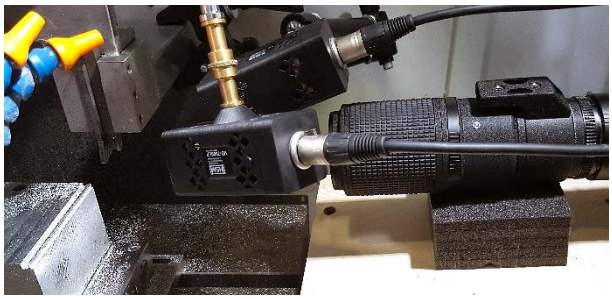

Fig. 1. High-speed camera setup.

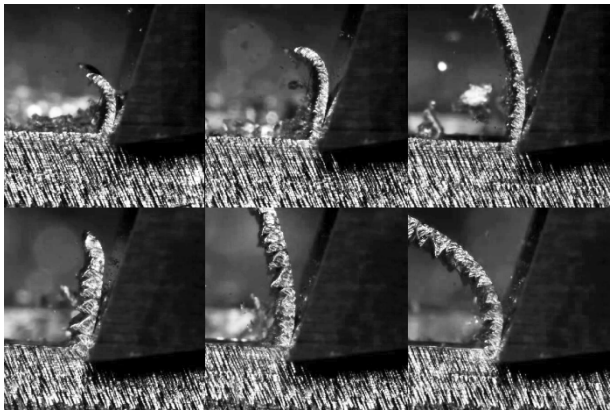

Fig. 2. Chip formation process. Images are extracted from high-speed recordings.

2.2 Force measurement

The cutting forces were measured with a multi-component dynamometer (Kistler 9129AA), an adherent multicomponent charge amplifier and a data acquisition device (National Instrument NI cDAQ-9178).

The cutting forces measured in the planning direction (x) and perpendicular (y) to it are plotted in Fig. 3-4. for various rake angle γ. Parameter a denotes the depth of cut.

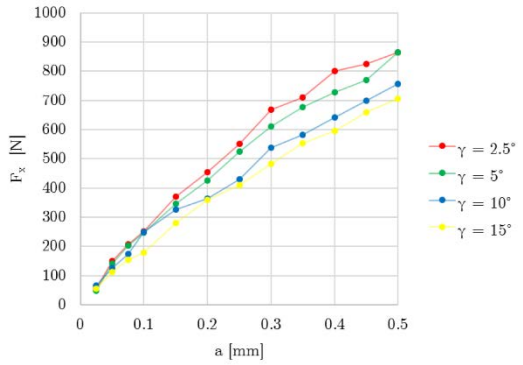

Fig. 3. Average cutting forces in direction *x*.

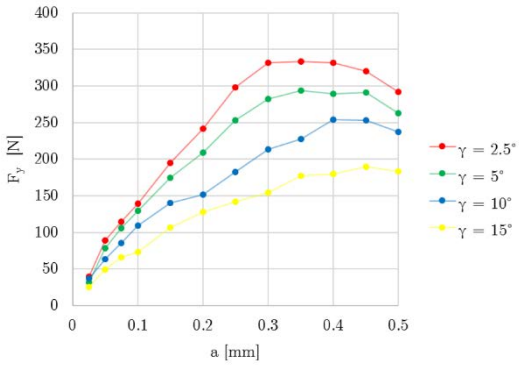

Fig. 4. Average cutting forces in direction *y*.

3. Finite element analysis

The planning process was simulated by two dimensional FE models using the commercial finite element software ABAQUS 2016.

Coupled thermo-mechanical analyses were carried out to include thermal effects. We used sacrificial layers to simulate the cutting mechanisms.

The material behavior was characterized by Johnson-Cook model, where the yield stress at non-zero strain rate is defined as

$$\bar{\sigma} = \left[A + B\left(\bar{\varepsilon}^{pl}\right)^{n}\right]\left[1 + C \cdot \ln\left(\frac{\dot{\bar{\varepsilon}}^{pl}}{\dot{\varepsilon}_0}\right)\right] \times \left[1 - \hat{T}^{m}\right]. \quad (0.1)$$

$\bar{\varepsilon}^{pl}$ denotes the equivalent plastic strain and A, B, n, C, $\dot{\varepsilon}_0$ and m are material parameters measured at or below the transition temperature T_t. The dimensionless temperature field $\hat{T}$ is defined as

$$\hat{T} \equiv \begin{cases} 0 & \text{for} \quad T < T_t \\ \dfrac{T - T_t}{T_m - T_t} & \text{for} \quad T_t \le T \le T_m \\ 1 & \text{for} \quad T > T_m \end{cases} \quad (0.2)$$

where T_m is the melting temperature. The Johnson-Cook dynamic failure model was applied in this analysis to determine the fracture initiation strain. The plastic strain at failure is calculated by

$$\bar{\varepsilon}_f^{pl} = \left[d_1 + d_2 \exp\left(-d_3\eta\right)\right]\left[1 + d_4 \ln\left(\frac{\dot{\bar{\varepsilon}}^{pl}}{\dot{\varepsilon}_0}\right)\right] \times \left[1 + d_5\hat{T}\right], \quad (0.3)$$

where $\eta = \mathrm{tr}(\boldsymbol{\sigma})/(3\bar{\sigma})$ is the stress triaxiality and $d_1 \ldots d_5$ are material parameters. Failure is assumed to occur when the damage parameter

$$\omega = \sum\left(\frac{\Delta\bar{\varepsilon}^{pl}}{\bar{\varepsilon}_f^{pl}}\right) \quad (0.4)$$

exceeds the critical value 1. Different damage evolution rules (linear, exponential) were tested in the simulations. The heat generated by the plastic dissipation and the friction was included in the model. The contact behavior of the tool-chip interface was modelled using modified Columb friction law.

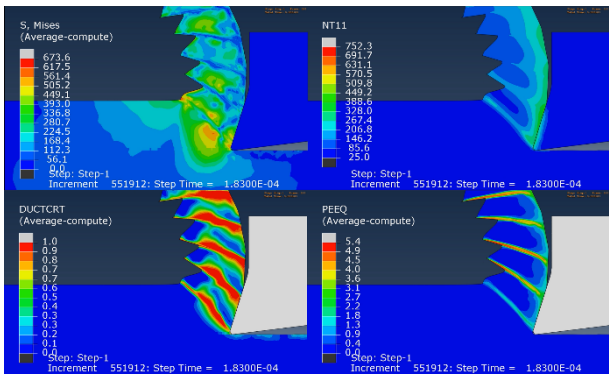

Fig. 5. Finite element simulation of the chip formation process.

Acknowledgements

The research leading to these results has received funding from the European Research Council under the European Union's Seventh Framework Programme (FP/2007-2013) / ERC Advanced Grant Agreement n. 340889.